"Omics" Prospective Monitoring of Bariatric Surgery: Roux-En-Y Gastric Bypass Outcomes Using Mixed-Meal Tolerance Test and Time-Resolved ^{1}H NMR-Based Metabolomics

Thiago I.B. Lopes,[1] Bruno Geloneze,[2] José C. Pareja,[2] Antônio R. Calixto,[2]
Márcia M.C. Ferreira,[1] and Anita J. Marsaioli[1]

Abstract

Roux-en-Y gastric bypass (RYGB) surgery goes beyond weight loss to induce early beneficial hormonal changes that favor glycemic control. In this prospective study, ten obese subjects diagnosed with type 2 diabetes underwent bariatric surgery. Mixed-meal tolerance test was performed before and 12 months after RYGB, and the outcomes were investigated by a time-resolved hydrogen nuclear magnetic resonance (^{1}H NMR)-based metabolomics. To the best of our knowledge, no previous omics-driven study has used time-resolved ^{1}H NMR-based metabolomics to investigate bariatric surgery outcomes. Our results presented here show a significant decrease in glucose levels after bariatric surgery (from 159.80 ± 61.43 to 100.00 ± 22.94 mg/dL), demonstrating type 2 diabetes remission ($p < 0.05$). The metabolic profile indicated lower levels of lactate, alanine, and branched chain amino acids for the operated subject at fasting state after the surgery. However, soon after food ingestion, the levels of these metabolites increased faster in operated than in nonoperated subjects. The lipoprotein profile achieved before and after RYGB at fasting was also significantly different, but converging 180 min after food ingestion. For example, the very low-density lipoprotein, low-density lipoprotein, N-acetyl-glycoproteins, and unsaturated lipid levels decreased after RYGB, while phosphatidylcholine and high-density lipoprotein increased. This study provides important insights on RYGB surgery and attendant type 2 diabetes outcomes using an "omics" systems science approach. Further research on metabolomic correlates of RYGB surgery in larger study samples is called for.

Introduction

OVERWEIGHT AND OBESITY ARE PREVENTABLE CONDITIONS defined as abnormal or excessive fat accumulation that may impair health. In fact, overweight and obesity are linked to more deaths worldwide than being underweight. In 2014, more than 1.9 billion adults were overweight. Of these, over 600 million were obese (WHO, 2015a). In addition to adults, obesity affects 42 million children (WHO, 2015b), and bariatric surgery is one of the most effective treatments for severe obese patients by allowing substantial weight loss and resolving obesity-associated comorbidities (Lima et al., 2010; Vasques et al., 2013).

Popular weight loss procedures are laparoscopic adjustable banding (41%), sleeve gastrectomy (66%), and gastric bypass (62%). Lifestyle, diet, and pharmacotherapies account for less than 10% excess weight loss (Khan et al., 2015). How-

ever, bariatric surgery is indicated only for patients with morbid obesity (body mass index [BMI] >40 kg/m^2) or in cases of moderate obesity associated with comorbidities, particularly the type 2 diabetes (Bruce and Mitchell, 2015; Lindeque et al., 2015).

Roux-en-Y gastric bypass surgery (RYGB) is one of the most common bariatric procedures that goes beyond weight loss and induces early beneficial hormonal changes favoring glycemic control (Vaurs et al., 2016). A meta-analysis shows that 76.8% of individuals undergoing bariatric surgery experienced complete remission of diabetes in an unexpectedly short amount of time (Buchwald et al., 2004).

Recently, a hydrogen nuclear magnetic resonance (^{1}H NMR) metabolomic profiling study showed alterations of basal metabolism among overweight diabetic subjects after RYGB, and these alterations were associated with energy homeostasis (decreased glucose and increased lactate and acetate levels),

[1]Chemistry Institute and [2]Laboratory of Investigation on Metabolism and Diabetes, State University of Campinas–UNICAMP, Campinas, São Paulo, Brazil.

decreased branched-chain amino acids (BCAA), and changes in lipid metabolism (Lopes et al., 2015). Similarly, mass spectrometry-based metabolomics applied to patients with RYGB (Laferrère et al., 2011; Lindqvist et al., 2013; Mutch et al., 2009) revealed that oral versus gastric mixed-meal tolerance test (MMTT) showed higher incretin and insulin responses after oral MMTT (Lindqvist et al., 2013). Laferrère et al. suggested that the enhanced decrease in circulating amino acids after RYGB is independent of weight loss and may contribute to glucose homeostasis observed after surgery (Laferrère et al., 2011). However, to the best of our knowledge, none of the previous studies has used time-resolved ^{1}H NMR to investigate bariatric surgery.

Therefore, the aim of this study was to prospectively monitor the metabolic responses of ten obese subjects before and 12 months after RYGB using a time-resolved ^{1}H NMR-based metabolomic approach. This approach consisted of measuring the metabolic profile after ingestion of a standard meal that provided complementary information to the "*static*" metabolomic approaches (Barding et al., 2012). Metabolomic studies frequently use chemometric methods as principal component analysis or partial least squares discriminant analysis (PLS-DA) to extract information from the analytical data. In this work, *N*-way partial least squares discriminant analysis (NPLS-DA) was used to take advantage of data structure, which can be considered trilinear (subjects × time × variables).

Materials and Methods

The study design

RYGB outcomes were monitored using MMTT and time-resolved ^{1}H NMR-based metabolomics. In short, plasma samples were collected before and 12 months after the bariatric surgery; these samples were analyzed by ^{1}H NMR providing the metabolic and lipoprotein profiles using a within-subject design in 10 obese subjects. Changes in the metabolic and lipoprotein profiles were investigated by chemometric tools.

Description of the study subjects

Subjects with obesity (levels II or III) and diagnosed with type 2 diabetes were recruited at "Clinical Hospital" from "State University of Campinas–UNICAMP." In this study, subjects with psychiatric disease; history of alcohol or drug abuse; cancer; cardiac, renal, or hepatic disease; insulin treatment; and uncontrolled blood pressure were excluded. Ten obese subjects that underwent RYGB surgery were selected, five of whom were women and five were men, with a total sample age range from 25 to 65 years old. The protocol was approved by the Institutional Review Board and the Brazilian Health Regulatory Agency. The data were collected according to the Good Clinical Practice Guidelines of the Declaration of Helsinki, and informed consent was obtained from all individuals. The number of registration at the National Institute of Health (NIH) is NCT00566189.

Mixed-meal tolerance test

The MMTT was conducted at 8:00 a.m. for subjects before and 12 months after RYGB. Venous blood samples were collected at 0, 15, 30, 45, 60, 90, 120, 150, and 180 min after a mixed meal. The total caloric value, fat, carbohydrate, and protein contents were as follows: 521.5 kcal, 31.6%, 49.4%, and 19%, respectively.

Plasma collection and storage

Blood samples were collected in Na$_2$EDTA (1.0 mg/mL) during the postprandial period. The plasma samples were obtained by centrifugation at 800 *g* for 15 min, and the aliquots were transferred to polypropylene tubes and stored at −80°C until they were assayed.

Sample preparation to ^{1}H NMR analysis

The plasma was thawed, and 400 μL of plasma was mixed with phosphate buffer prepared in deuterium oxide [200 μL; pH = 7.4; 50 mM with 1.0 mM of *2,2,3,3-d$_4$-3*-(trimethylsilyl) propionic acid (TMSP) and 5.0 mM of sodium formate]. The samples were homogenized and centrifuged (10,000 *g* for 20 min at 4°C) to remove any particles in suspension. Finally, part of the supernatant (500 μL) was transferred to 5-mm NMR tubes. Duplicates of all samples were prepared, yielding a total of 360 samples.

Acquisition and processing of the ^{1}H NMR spectra

The experiments were performed without spinning at 298 K using a Bruker Avance III of 9.4 T (400.1819 MHz, ^{1}H frequency) spectrometer equipped with a 5 mm TBI probe. Both T$_2$-edited and diffusion-edited ^{1}H NMR spectra were acquired for each sample. The T$_2$-edited ^{1}H NMR spectra were acquired with Carr–Purcell–Meiboom–Gill pulse sequence (CPMG) to suppress plasma protein, and lipoprotein signals with T$_2$. PRESAT was used to suppress the water signal. The following parameters were applied: 300 μsec of evolution time and 600 msec of total spin–spin relaxation delay and 64 scans. The magnetic field homogeneity was optimized for each sample. The diffusion-edited ^{1}H NMR spectra were acquired by bipolar pulse pair-longitudinal eddy current delay pulse sequence that was intended to suppress signals from molecules with large diffusion coefficients, which are the small molecules. The WATERGATE 3-9-19 pulse sequence was used to suppress the water signal. A sine-shaped gradient pulse of 90% maximum strength, with 2.0 msec of duration (little delta), followed by a delay (big delta) of 100 msec that allowed the eddy currents to decay, was applied in the spectra acquisition. The delay for the binomial water suppression was set at 17.0 μsec, the gradient pulse was 1.0 msec, and the spectra were acquired with 32 scans. For both pulse sequences, the remaining acquisition parameters were as follows: spectral width, 6.0 kHz; data size, 32 k; acquisition time, 2.73 sec; constant receiver gain, 203; and relaxation delay, 5.0 sec. The data processing included zero filling to 128 k, line-broadening multiplication by 1.0 (T$_2$-edited ^{1}H NMR) and 3.0 Hz (diffusion-edited ^{1}H NMR), and Fourier transformation. All of the spectra were phase and baseline corrected and referenced to TMSP at 0.000 ppm (T$_2$-edited ^{1}H NMR) and to the methyl resonance of lipoproteins at 0.800 ppm (diffusion-edited ^{1}H NMR) using TopSpin software (v3.1; Bruker BioSpin). Typical full spectra are presented as Supplementary Data (Supplementary Figs. S1 and S2).

NMR peak assignment was performed by means of literature data (Bell et al., 1987; Fan, 1996; Foxall et al., 1993) and confirmed with heteronuclear single quantum coherence

spectroscopy (2D ^{1}H-^{13}C HSQC) and selective homonuclear total correlation spectroscopy (selective 1D ^{1}H-^{1}H TOCSY) using Bruker's available sequences.

Preprocessing data

The T_2-edited and diffusion-edited ^{1}H NMR spectra were individually aligned with the MATLAB ICOSHIFT tool (Savorani et al., 2010) using the signal of sodium formate (for T_2-edited ^{1}H NMR) and methyl resonance (for the diffusion-edited ^{1}H NMR) as the shift reference. TMSP was not used in this case as reference due to its interaction with the albumin present in plasma (Kriat et al., 1992). To reduce the huge dimension of data, the *optimized bucketing algorithm* was used (Sousa et al., 2013). The initial size of each bucket was set to 0.004 ppm, and the slackness was adjusted to 50%. The spectra ensembles of before and after the ICOSHIFT alignment and Sousa's bucket are in the Supplementary Data (Supplementary Figs. S3 and S4). The two resulting data sets were separately arranged in a ''cube'' format of dimensions ($I \times J \times K$). The cubes are formed by $i = 1,2, \ldots, I$ samples; $j = 1,2, \ldots, J$ time intervals; and $k = 1,2, \ldots K$ buckets. Their final dimensions are $40 \times 9 \times 908$ for T_2-edited ^{1}H NMR data and $40 \times 9 \times 833$ for diffusion-edited ^{1}H NMR. For validation purpose, both data sets were divided into training and test sets containing 2/3 and 1/3 of the samples, respectively. These two sets were obtained by using a distance-based optimal routine designed for MATLAB (Marengo and Todeschini, 1992).

Data analysis

The NPLS-DA was used to differentiate the patients before and after RYGB, the analysis was performed in N-way toolbox for MATLAB (Andersson and Bro, 2000). This chemometric method is described in the Supplementary Data (Supplementary Fig. S5). A model was constructed using a training set, and the number of factors was determined by cross validation, using 28 randomly chosen segments, and validated by prediction of 12 independent samples (validation set). The NPLS-DA was performed on mean-centered spectral profiles using a Y-matrix corresponds to a dummy matrix of the classes (containing 0 and 1) (Bro, 1996). The number of latent variables were determined by cross-validation procedure on the training set and validated by the test set. To achieve the relative concentrations of the main lipoprotein fractions, multivariate curve resolution (MCR) was used with methyl resonances from diffusion-edited ^{1}H NMR spectra. An alternating least squares algorithm was applied with non-negativity and unimodality constraints. Initial spectra estimates were obtained by deconvolution of a spectrum model (Otvos et al., 1991a, 1991b).

Results

All ten patients who underwent RYGB showed a significant decrease in BMI (from 32.38 ± 2.11 to 25.48 ± 1.85 kg/m^2, $p < 0.001$), glucose level (from 159.80 ± 61.43 to 100.00 ± 22.94 mg/dL, $p = 0.010$), and homeostasis mode assessment insulin resistance (from 10.961 ± 8.314 to 1.089 ± 0.526, $p = 0.002$), thus demonstrating overall weight loss and remission of diabetes 12 months after the bariatric surgery ($p < 0.05$). Others clinical information about the subjects and metabolic alterations associated with the basal metabolism can be found in Lopes et al. (2015). In this study, the time-resolved ^{1}H NMR-based metabolomic approach was used to expand the ''*static*'' information normally provided by metabolomic studies. The RYGB-associated changes were highlighted by NPLS-DA, and the respective metabolites were assigned. Figure 1 shows model spectrum used in this study to access the metabolic and lipoprotein profile, and RYGB-associated compounds are assigned in Table 1.

NPLS-DA model from T_2-edited ^{1}H NMR data

The root mean squared error of the NPLS-DA model calibration and cross validation from T_2-edited ^{1}H NMR data revealed that two factors were significant, and these explained 24.72% and 55.17% of the variance in the X (variables) and Y (response) blocks, respectively. Although the model explained a relatively low amount of variance, it discriminated the samples before and after 12 months RYGB (Fig. 2A). Only four (14.28%) samples were mispredicted in the calibration set, and two errors (16.67%) occurred when using the prediction set to validate the model.

Samples from patients after RYGB showed relatively negative scores for factors associated with alterations in the T_2-edited ^{1}H NMR spectra, as shown in Figure 2B. The alterations observed in the spectral loadings were connected to the variations in BCAA, alanine, lactate, and glucose concentrations. The temporal loading represents the variation of metabolic responses during the postprandial period (Fig. 2C). The metabolic profile reached a maximum ~ 15 min after the meal and returned to baseline with small fluctuations after 60 min due to the anabolic process.

NPLS-DA model from diffusion-edited ^{1}H NMR data

The root mean squared error of calibration and cross validation revealed two significant factors for the NPLS-DA model that explained 41.81% and 53.09% of the variance in the X and Y blocks, respectively. Samples from patients 12 months after RYGB showed relatively negative scores (Fig. 3A). The main observed alterations are explained by spectral loading from diffusion-edited ^{1}H NMR spectra (Fig. 3B), indicating alterations in unsaturated lipids, N-acetyl glycoproteins, phosphatidylcholine, and lipoprotein levels. The temporal loading showed the MMTT lipoprotein response by revealing a slight increase in the lipoprotein level 15 min after the meal that remained high for 150 min with small fluctuations. After this time, an abrupt decrease was observed (Fig. 3C). Finally, the NPLS-DA model from the diffusion-edited ^{1}H NMR data was reasonably accurate. Two errors (7.14%) occurred in the calibration set, and two samples were wrongly predicted (16.67%) when validating the model with the test set. With the aim of obtaining more detailed information from the lipoprotein profile, MCR was applied to the methyl resonances providing the relative concentrations of low-density lipoprotein (LDL), very low-density lipoprotein (VLDL), and high-density lipoprotein (HDL) (Supplementary Fig. S6).

Discussion

In the present study, the NPLS-DA chemometric analysis was successful in integrating chemical information from time-resolved ^{1}H NMR-based metabolomic approach, providing an extremely large and unbiased overview of the mixed-meal tolerance response in individuals that underwent
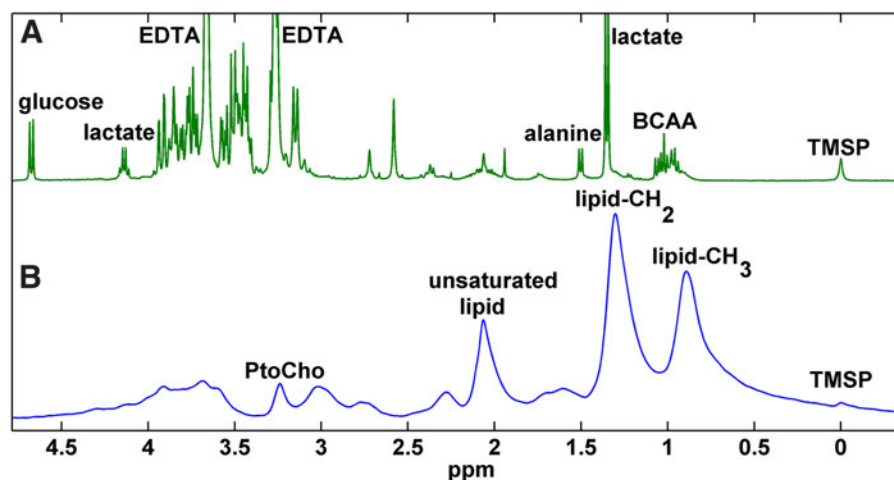
FIG. 1. (A) T_2-edited and (B) diffusion-edited ^{1}H NMR spectrum model for overweight subjects before RYGB. ^{1}H NMR, hydrogen nuclear magnetic resonance; RYGB, Roux-en-Y gastric bypass.

RYGB. These results should be placed into context from a biochemical point of view in particular.

Alterations in energy metabolism

After meals, glucose levels nearly doubled among patients who had undergone RYGB, while before bariatric surgery, glucose levels increased only 50% compared to baseline levels (Fig. 4A). These observations are consistent with the physiology of gastric bypass surgery, which involves a gut "*shortcut*" that facilitates glucose absorption (Buchwald and Oien, 2013). Glucose levels remain high for 45 min, and they decrease more quickly among patients who have undergone surgery. This change may be related to the fact that RYGB affects the enteroinsular axis by allowing food to reach the ileum before it is completely digested, which stimulates the secretion of the hormones GLP-1 (glucagon-like peptide-1) and GIP (gastric inhibitory polypeptide). High levels of these hormones are directly associated with lower glucose levels, lower insulin levels, and glucagon suppression (Rubino et al., 2006; Thaler and Cummings, 2009). Considering the areas under the curve, the glucose levels are low among patients who have undergone surgery, contributing to the normalization of blood glucose and the remission of type 2 diabetes.

The lactate concentration also decreased significantly after RYGB, with similar fluctuations observed for glucose ($p < 0.001$). The maximum lactate concentration was achieved 15 min after food ingestion, and it remained elevated for 90 min (Fig. 4B). The initial increase and subsequent decrease in the lactate concentration may be related to the availability of glucose as an energy source. After food ingestion, the glucose concentration is high, inhibiting gluconeogenesis, which contributes to high lactate levels. Glucose consumption displaces lactate to the gluconeogenesis process. After RYGB, a decrease in BCAA (valine, leucine, and isoleucine) and alanine levels contributed to the remission of type 2 diabetes (Lee et al., 2016;

TABLE 1. ASSIGNMENT OF HIGHLIGHTED RESONANCES IN THE T_2-EDITED AND DIFFUSION-EDITED ^{1}H NMR SPECTRUM

Metabolite	Spectra edited by	Alteration after RYGB	δ ^{1}H (ppm)	Assignment	J (Hz)
HDL	Diffusion	Increase	0.77	-CH$_3$	—
			~1.21	(CH$_2$)$_n$	—
LDL	Diffusion	Decrease	0.82	-CH$_3$	—
			~1.24	(CH$_2$)$_n$	—
VLDL	Diffusion	Decrease	0.88	-CH$_3$	—
			~1.26	(CH$_2$)$_n$	—
Isoleucine	T_2	Decrease	0.93 (t)	δ-CH$_3$	7.1
			0.99 (d)	β-CH$_3$	7.0
Leucine	T_2	Decrease	0.95 (d)	δ-CH$_3$	7.0
			0.96 (d)	δ-CH$_3$	7.0
Valine	T_2	Decrease	0.97 (d)	-CH$_3$	7.0
			1.02 (d)	-CH$_3$	7.0
Lactate	T_2	Decrease	1.32 (d)	-CH$_3$	7.0
			4.12 (q)	-CH-	7.0
Unsaturated lipid	Diffusion	Decrease	1.85	-CH=CH-	—
N-acetyl-glycoproteins	Diffusion	Decrease	2.02	-CH$_3$	—
Phosphatidylcholine	Diffusion	Increase	3.20	-CH$_3$	—
β-Glucose	T_2	Decrease	4.63 (d)	Hα	8.0

HDL, high-density lipoprotein; LDL, low-density lipoprotein; RYGB, Roux-en-Y gastric bypass; VLDL, very low-density lipoprotein.
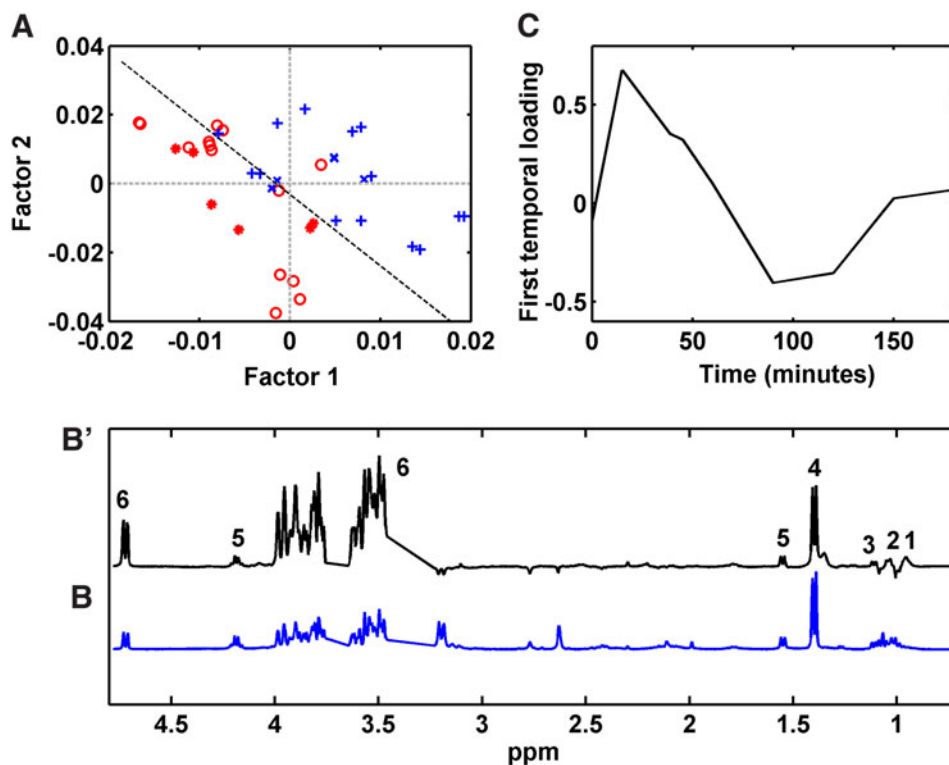
FIG. 2. **(A)** Scores plot for two first factors of the NPLS-DA model from T_2-edited ^{1}H NMR data; **(B')** first spectral loading from NPLS-DA model; **(B)** T_2-edited ^{1}H NMR spectra model; and **(C)** first temporal loading from NPLS-DA model. 1, isoleucine; 2, leucine; 3, valine; 4, lactate; 5, alanine; and 6, glucose. Calibration samples from patients (+) before and (o) after RYGB. Validation samples from patients (x) before and (*) after RYGB. NPLS-DA, *N*-way partial least squares discriminant analysis.
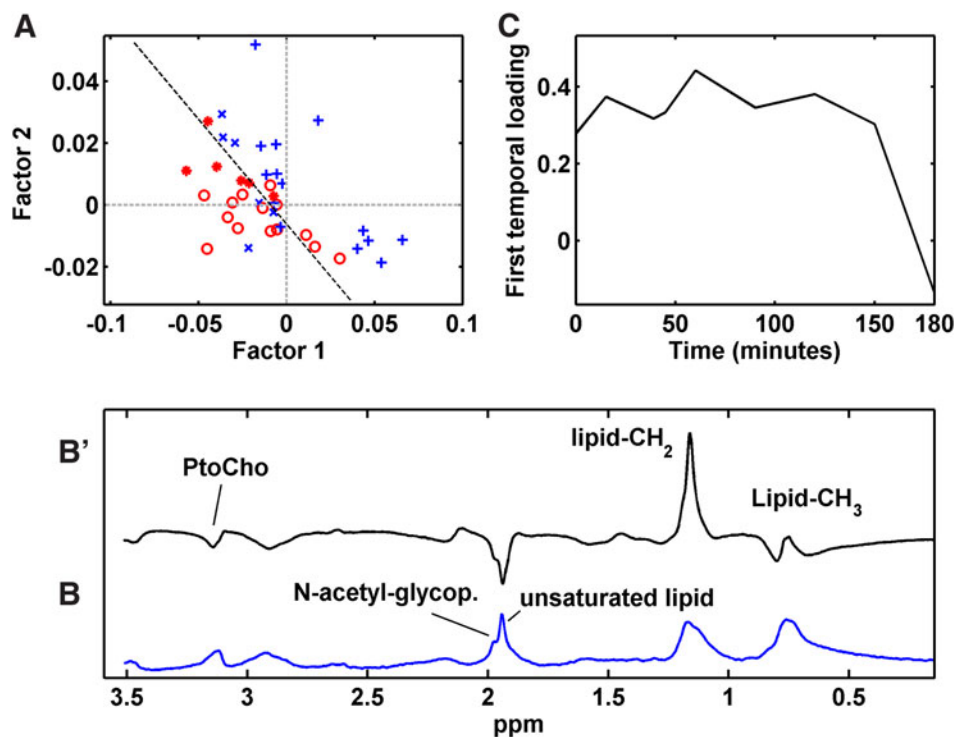

FIG. 3. **(A)** Scores plot for two first factors of the NPLS-DA model from diffusion-edited ^{1}H NMR data; **(B')** first spectral loading from the NPLS-DA model; **(B)** diffusion-edited ^{1}H NMR spectra model; and **(C)** first temporal loading of the NPLS-DA model. Calibration samples from patients (+) before and (o) after RYGB. Validation samples from patients (x) before and (*) after RYGB. PtoCho, phosphatidylcholine.
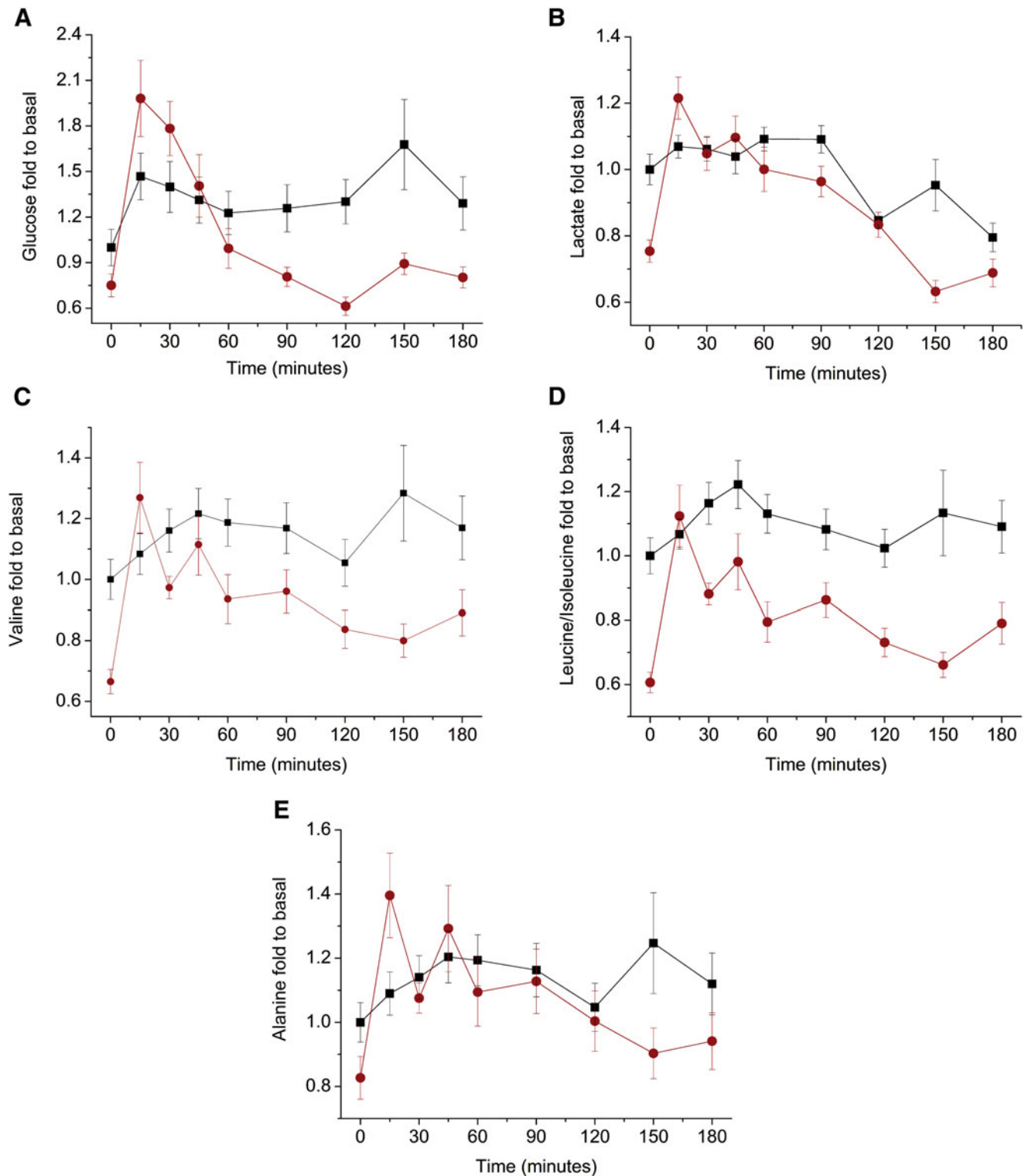
FIG. 4. Trajectories of the postprandial states, shown as fold changes compared to the baseline levels of **(A)** glucose; **(B)** lactate; **(C)** valine; **(D)** leucine/isoleucine; and **(E)** alanine. (■) before and (●) after RYGB.

Newgard et al., 2009). The postprandial effect of increasing concentrations of valine (Fig. 4C), isoleucine, and leucine (Fig. 4D) is more rapid in patients after RYGB and it remains high for 60 min. The levels of isoleucine and leucine are considered together due to spectral overlapping. The results show a significant decrease in BCAA after surgery ($p < 0.001$), which is in agreement with previously reported data (Jung et al., 2012; Laferrère et al., 2011). Alanine levels were also significantly lower after RYGB (Fig. 4E) ($p < 0.001$), although to a lesser extent than those of BCAA.
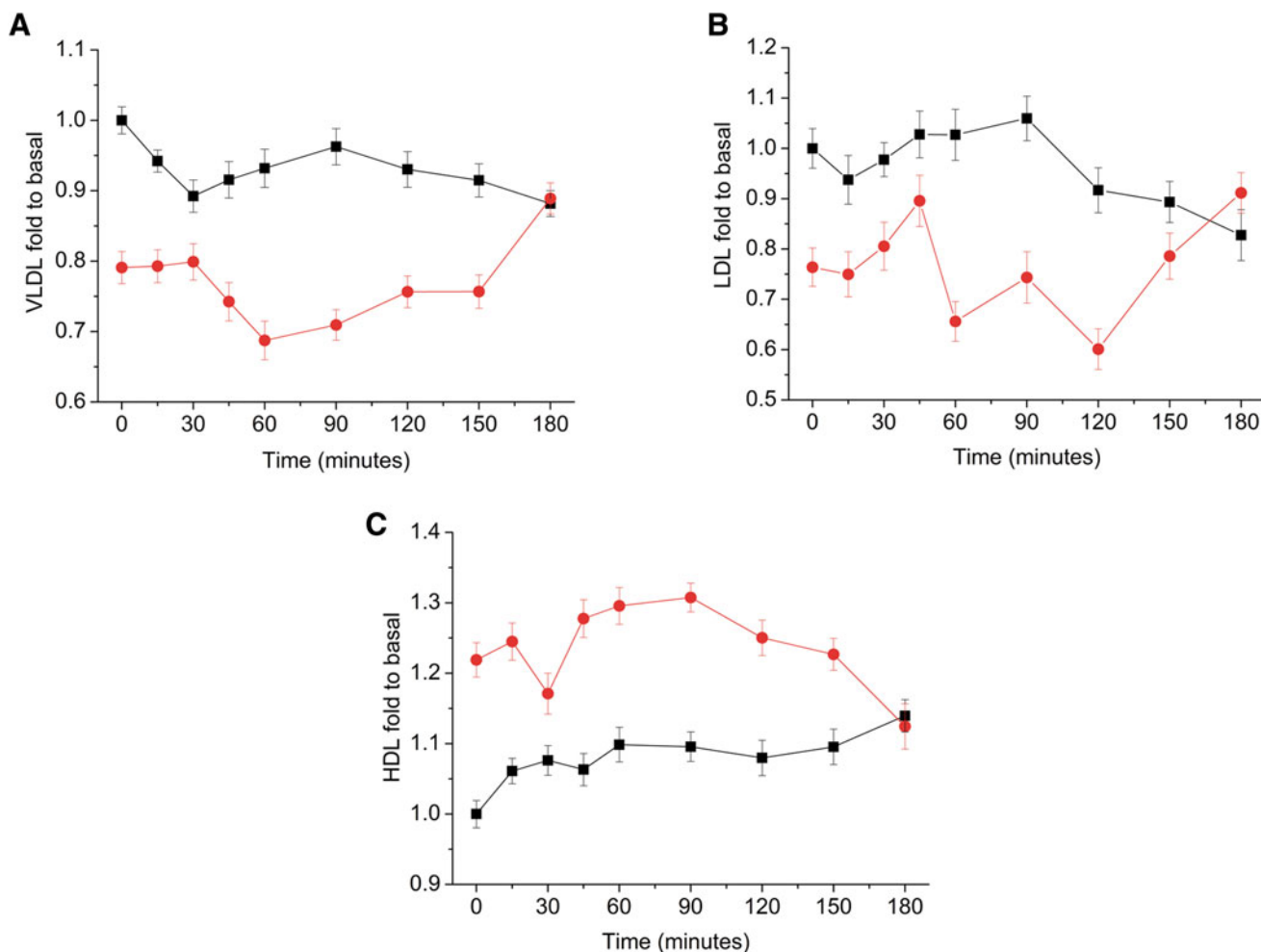
FIG. 5. Trajectories of the postprandial states, shown as fold changes compared to the baseline levels of **(A)** VLDL; **(B)** LDL; and **(C)** HDL. (■) before and (●) after RYGB. HDL, high-density lipoprotein; LDL, low-density lipoprotein; VLDL, very low-density lipoprotein.

Alterations of the lipoprotein profile

^{1}H NMR can evaluate lipoproteins and chylomicrons triglyceride contents in blood samples by surveying physical phenomena such as diffusion and rotational motion (Simmler et al., 2014). Due to the spectral signal overlap, direct quantification is impossible, and deconvolution or chemometric methods are used for final visualization. In this work, MCR was applied to methyl resonances from diffusion-edited ^{1}H NMR spectra to provide the relative VLDL, LDL, and HDL concentrations (Supplementary Fig. S7). Twelve months after RYGB, the VLDL and LDL levels significantly decreased (Fig. 5A, B) ($p < 0.001$), while the phosphatidylcholine and HDL (Fig. 5C) levels increased during the MMTT. The profile from patients before and after RYGB converged 180 min after food ingestion, indicating normalization of the lipoprotein profile.

The results show higher levels of phosphatidylcholine and lower levels of N-acetyl-glycoproteins after RYGB, which could indicate lipid mobilization from nonadipose tissues associated with weight loss and reduction of inflammatory processes. However, decreasing unsaturated lipid levels could indicate excessive lipid peroxidation or oxidative stress

after bariatric surgery. The oxidative stress theory is corroborated by the increase of lactate level in the metabolic profile (Richard and Bradford, 2009).

Conclusion

The combination of ^{1}H NMR and chemometric analysis was successfully applied to monitor the mixed-meal tolerance in individuals that underwent RYGB, leading to a broader "omics" system science view of the MMTT response. Time-resolved ^{1}H NMR-based metabolomic approach provided complementary information to the "*static*" metabolomics and contributed to the development of surgical and nonsurgical treatments of obesity/overweight subjects. The RYGB outcomes show a profound impact of the surgery on BCAA, alanine, lactate, and glucose metabolism. The absorption of glucose is faster after gastric bypass, but the smaller total glucose is absorbed, and it contributes to a smaller level of plasmatic glucose in the operated subject 1 h after food ingestion. A similar alteration was observed for lactate as glucose availability affects the lactate concentration through the gluconeogenesis process. The postprandial BCAA concentrations increase quickly among patients who

underwent the surgery, but these levels decreased significantly in 45 min. With regard to the lipoprotein profile, decreases in VLDL, LDL, N-acetyl glycoproteins, and unsaturated lipids were observed. HDL and phosphatidylcholine levels increased. The profile from patients before and after RYGB converged after 180 min, signaling a normalization of the lipoprotein profile.

Notwithstanding the modest sampling size, this study has demonstrated a marked change of the metabolic and lipoprotein response to MMTT, thereby providing valuable system-based information about RYGB outcomes. Further research on metabolomic correlates of RYGB surgery in larger study samples is called for.

Acknowledgments

Author Disclosure Statement

The authors declare that no competing financial interests exist.

References

Andersson CA, and Bro R. (2000). The N-way Toolbox for MATLAB. Chemometr Intell Lab Syst 52, 1–4.

Barding GA, Salditos R, and Larive CK. (2012). Quantitative NMR for bioanalysis and metabolomics. Anal Bioanal Chem 404, 1165–1179.

Bell JD, Brown JC, Nicholson JK, and Sadler PJ. (1987). Assignment of resonances for 'acutephase' glycoproteins in high resolution proton NMR spectra of human blood plasma. FEBS Lett 215, 311–315.

Bro R. (1996). Multiway calibration: multilinear PLS. J Chemometrics 10, 47–61.

Bruce DM, and Mitchell AL. (2015). Surgery for obesity. Medicine 43, 101–103.

Buchwald H, Avidor Y, Braunwald E, et al. (2004). Bariatric surgery: a systematic review and meta-analysis. JAMA 292, 1724–1737.

Buchwald H, and Oien DM. (2013). Metabolic/bariatric surgery worldwide 2011. Obes Surg 23, 427–436.

Fan TWM. (1996). Metabolite profiling by one- and two-dimensional NMR analysis of complex mixtures. Prog Nucl Magn Res Spec 28, 161–219.

Foxall PJ, Spraul M, Farrant RD, Lindon LC, Neild GH, and Nicholson JK. (1993). 750 MHz ^{1}H-NMR spectroscopy of human blood plasma. J Pharm Biomed Anal 11, 267–276.

Jung JY, Kim IY, Kim YN, et al. (2012). ^{1}H NMR-based metabolite profiling of diet-induced obesity in a mouse mode. BMB Rep 45, 419–424.

Khan S, Rock K, Baskara A, Qu W, Nazzal M, and Ortiz J. (2015). Trends in bariatric surgery from 2008 to 2012. Am J Surg 211, 1041–1046.

Kriat M, Gouny SC, Dury JV, Sciaky M, Viout P, and Cozzone PJ. (1992). Quantitation of metabolites in human blood serum by proton magnetic resonance spectroscopy. A comparative study of the use of formate and TSP as concentration standards. NMR Biomed 5, 179–184.

Laferrère B, Reilly D, Arias S, et al. (2011). Differential metabolic impact of gastric bypass surgery versus dietary intervention in obese diabetic individuals despite identical weight loss. Sci Transl Med 3, 80–82.

Lee CC, Watkins SM, Lorenzo C, et al. (2016). Branched-chain amino acids and insulin metabolism: the insulin resistance atherosclerosis study (IRAS). Diabetes Care 39, 582–588.

Lima MM, Pareja JC, Alegre SM, et al. (2010). Acute effect of roux-en-y gastric bypass on whole-body insulin sensitivity: a study with the euglycemic-hyperinsulinemic clamp. J Clin Endocrinol Metab 95, 3871–3875.

Lindeque JZ, van Rensburg PJJ, Louw R, et al. (2015). Obesity and metabolomics: metallothioneins protect against high-fat diet-induced consequences in metallothionein knockout mice. OMICS 19, 92–103.

Lindqvist A, Spégel P, Ekelund M, Mulder H, Hedenbro LGJ, and Wierup N. (2013). Effects of ingestion routes on hormonal and metabolic profiles in gastric-bypassed humans. J Clin Endocrinol Metab 98, 856–861.

Lopes TIB, Geloneze B, Pareja JC, Calixto AR, Ferreira MMC, and Marsaioli AJ. (2015). Blood metabolome changes before and after bariatric surgery: A ^{1}H NMR-based clinical investigation. OMICS 19, 318–327.

Marengo E, and Todeschini R. (1992). A new algorithm for optimal, distance-based experimental design. Chemometr Intell Lab Syst 16, 37–44.

Mutch DM, Fuhrmann JC, Rein D, et al. (2009). Metabolite profiling identifies candidate markers reflecting the clinical adaptations associated with Roux-en-Y gastric bypass surgery. PLoS One 4, e7905.

Newgard CB, An J, Bain JR, et al. (2009). A branched-chain amino acid-related metabolic signature that differentiates obese and lean humans and contributes to insulin resistance. Cell Metab 9, 311–326.

Otvos JD, Jeyarajah EJ, and Bennett DW. (1991a). Quantification of plasma lipoproteins by proton nuclear magnetic resonance spectroscopy. Clin Chem 37, 377–386.

Otvos JD, Jeyarajah EJ, Hayes LW, Freedman DS, Janjan NA, and Anderson TR. (1991b). Relationships between the proton nuclear magnetic resonance properties of plasma lipoproteins and cancer. Clin Chem 37, 369–376.

Richard JB, and Bradford JC. (2009). Relationship between blood lactate and oxidative stress biomarkers following acute exercise. Open Sports Med J 3, 44–48.

Rubino F, Forgione A, Cummings DE, et al. (2006). The mechanism of diabetes control after gastrointestinal bypass surgery reveals a role of the proximal small intestine in the pathophysiology of type 2 diabetes. Ann Surg 244, 741–749.

Savorani F, Tomasi G, and Engelsen SB. (2010). Icoshift: a versatile tool for the rapid alignment of 1D NMR spectra. J Magn Reson 202, 190–202.

Simmler C, Napolitano JG, McAlpine JB, Chen SN, and Pauli GF. (2014). Universal quantitative NMR analysis of complex natural samples. Curr Opin Biotechnol 25, 51–59.

Sousa SAA, Magalhães A, and Ferreira MMC. (2013). Optimized bucketing for NMR spectra: three case studies. Chemometr Intell Lab Syst 122, 93–102.

Thaler JP, and Cummings DE. (2009). Minireview: Hormonal and metabolic mechanisms of diabetes remission after gastrointestinal surgery. Endocrinology 150, 2518–2525.

Vasques ACJ, Pareja JC, Oliveira MS, et al. (2013). β-Cell function improvements in grade I/II obese subjects with type 2 diabetes 1 month after biliopancreatic diversion: results

from modeling analyses of oral glucose tolerance tests and hyperglycemic clamp studies. Diabetes Care 36, 4117–4124.

Vaurs C, Brun JF, Bertrand M, et al. (2016). Post-prandial hypoglycemia results from a non-glucose-dependent inappropriate insulin secretion in Roux-en-Y gastric bypassed patients. Metabolism 65, 18–26.

(WHO) World Health Organization. (2015a). Overweight and obesity: adults aged 18+. www.who.int/gho/ncd/risk_factors/overweight_text/en/ Accessed January 14, 2016.

(WHO) World Health Organization. (2015b). Obesity and overweight, Fact sheet No. 311. www.who.int/mediacentre/factsheets/fs311/en Accessed January 14, 2016.

Address correspondence to:
Prof. Anita J. Marsaioli, PhD
Chemistry Institute
Universidade Estadual de Campinas–UNICAMP
Campinas 13083-970
São Paulo
Brazil

E-mail: anita@iqm.unicamp.br

Abbreviations Used	
^{1}H NMR	= hydrogen nuclear magnetic resonance
BCAA	= branched-chain amino acid
BMI	= body mass index
CPMG	= Carr–Purcell–Meiboom–Gill pulse sequence
GIP	= gastric inhibitory polypeptide
GLP-1	= glucagon-like peptide-1
HDL	= high-density lipoprotein
LDL	= low-density lipoprotein
MCR	= multivariate curve resolution
MMTT	= mixed-meal tolerance test
NPLS-DA	= *N*-way partial least squares discriminant analysis
PtoCho	= phosphatidylcholine
RYGB	= Roux-en-Y gastric bypass
TMSP	= *2,2,3,3-d_4-3-*(trimethylsilyl) propionic acid
TOCSY	= homonuclear total correlation spectroscopy
VLDL	= very low-density lipoprotein